(s, 6 H, OCH_3), 2.23-4.40 (m, 16 H, NCH_2, OCH_2), 3.11 (d, 2 H, J = 13.2 Hz, $ArCH_2N$), 4.09 (d, 2 H, J = 13.2 Hz, $ArCH_2N$), 7.00 (d, 2 H, J_m = 1.5 Hz, ArH), 7.15 (d, 2 H, J_m = 1.5 Hz, ArH), 7.34 (s, 2 H, ArH).

What is probably **5**·I^+I^- gave the following: ^1H NMR ($CDCl_3$) δ 2.35 (s, 6 H, $ArCH_3$), 2.46 (s, 3 H, $ArCH_3$), 2.62 (s, 3 H, OCH_3), 3.31 (s, 6 H, OCH_3), 2.96-3.87 (m, 16 H, NCH_2, OCH_2), 4.22 (d, 2 H, J = 13.2 Hz, $ArCH_2N$), 4.34 (d, 2 H, J = 13.2 Hz, $ArCH_2N$), 7.15 (d, 2 H, ArH), 7.19 (d, 2 H, ArH), 7.26 (s, 2 H, ArH); FABMS (xenon ionization, 0 °C), 687 (M + I^+, 0.6), 561 (M + H^+, 100), 583 (M + Na^+, 21).

Crystal Structures. Compounds **5**·Na^+, **8**·Na^+, **8**·K^+, **8**·Cs^+, and 9 are crystallized in the monoclinic system in space groups $P2_1/n$, Cc, $P2_1/c$, $P2_1/c$ and $P2_1/m$, respectively. Unit cell dimensions are as follows: **5**·Na^+ a = 19.919 (2) Å, b = 14.725 (2) Å, c = 21.387 (2) Å, β = 111.85 (3)°, Z (the number of molecules in the unit cell) = 4; **8**·Na^+ a = 16.907 (6) Å, b = 12.543 (4) Å, c = 20.860 (7) Å, β = 117.89 (3)°, Z = 4; **8**·K^+ a = 14.078 (4) Å, b = 11.367 (3) Å, c = 25.909 (7) Å, β = 101.48 (2)°, Z = 4; **8**·Cs^+ a = 11.329 (3) Å, b = 14.364 (5) Å, c = 26.219 (10) Å, β = 105.03 (3)°, Z = 4; **9** a = 15.605 (11) Å, b = 15.799 (7) Å, c = 15.023 (7) Å, β = 94.43 (5)°, Z = 4 (two crystallographically unrelated molecules each having a mirror plane through the molecule are found in this unit cell). Compounds **6**·K^+, **14**, and **15** crystallize in the orthorhombic system in space groups $Pnma$, $P2_1na$ and $Pnma$, respectively. Unit cell dimensions are as follows: **6**·K^+ a = 21.210 (9) Å, b = 14.745 (6) Å, c = 11.808 (5) Å, Z = 4 (the molecule contains a crystallographic mirror plane); **14** a = 11.318 (3) Å, b = 7.835 (1) Å, c = 37.230 (8) Å, Z = 4; **15** a = 16.056 (4) Å, b = 15.370 (4) Å, c = 14.640 (3) Å, Z = 4 (the molecule contains a crystallographic mirror plane). With the exception of **6**·K^+ and **5**·Na^+, which were examined on a modified Picker FACS1 diffractometer, all measurements were taken on a Syntex $P\bar{1}$ diffractometer. All measurements except for those of **15**, which involved Cu Kα radiation, made use of Mo Kα radiation. Measurements were made at ambient temperature except for 9 and **14**, which were made at 115 K. Refinement of the eight structures gave R values currently at **5**·Na^+ 0.16, **6**·K^+ 0.08, **8**·Na^+ 0.06, **8**·K^+ 0.14, **8**·Cs^+ 0.08, 9 0.08, **14** 0.08, and **15** 0.08. All but **8**·Cs^+, which was solved by using heavy atom methods, were solved by using direct methods. Full details will be published elsewhere.

Host-Guest Complexation. 39. Cryptahemispherands Are Highly Selective and Strongly Binding Hosts for Alkali Metal Ions[1]

Donald J. Cram* and Siew Peng Ho

Contribution from the Department of Chemistry and Biochemistry, University of California, Los Angeles, California 90024. *Received October 15, 1985*

Abstract: The association constants (K_a, M^{-1}) and free energies of binding ($-\Delta G°$, kcal mol^{-1}) have been measured at 25 °C in $CDCl_3$ saturated with D_2O for cryptahemispherands **1-3**, cryptands **9-11**, and diazahemispherand **4** binding the alkali metal picrate salts. Methods were used in which complexes whose K_a values had been determined were equilibrated with hosts of unknown values. The equilibrium points were determined by ^1H NMR spectral methods. The cryptahemispherands as a class were found to be more powerful complexing agents than the cryptands. The two classes exhibited comparable ion selectivities. Plots of the $-\Delta G°$ values of the cryptands in $CDCl_3$-D_2O vs. those in 95% CH_3OH-5% H_2O were linear. The $-\Delta G°$ values for eight different sets of binding partners in $CDCl_3$-D_2O were found to be 5.2 ± 0.4 kcal mol^{-1} higher than the corresponding eight values in CH_3OH-H_2O. The results are discussed in terms of the relative states of preorganization for binding and desolvation of the various host classes.

The previous paper in this series reports the syntheses and crystal structures of complexes whose hosts belong to a new subclass called the cryptahemispherands, whose bicyclic structures are illustrated by **1-3**. The monocyclic diazahemispherand **4** was also prepared for purposes of comparison.[2] Hosts **1-3** combine certain structural features of the spherands (**5-7**),[3,4] the hemispherands (e.g., **8**),[5] and the cryptands (**9-11**),[6-8] which in turn are relatives of the chorands (e.g., **12**).[9] The trisanisyl molecular modules of **1-8** and the tetraanisyl module of reference compound **13**[10] are organized for binding during their syntheses rather than during the act of complexation. In these modules, the unshared electron pairs of the oxygens face inward toward the cavity, and their attached methyl groups are oriented outward, shielding the oxygens from solvation. In contrast, the $(CH_2OCH_2)_m$ and $(CH_2)_3N$ modules of **1-4** and **8-12** are conformationally mobile. The unshared electron pairs of their heteroatoms can face outward to be solvated or inward toward solvent parts occupying the cavity. The methylene groups can turn inward to fill the cavity or outward when the cavity is filled. Upon complexation with cations, the guest must conformationally reorganize these chains and displace solvent bound to their heteroatoms in the process.[3] The chorands, and particularly the cryptands, are *preorganized* for binding with respect to the sequences of their atoms but not with regard to their conformations or competitive complexation with solvent. The spherands are *preorganized* with respect to their atomic sequences, their conformations, and the unsolvated states of their heteroatoms.

This paper reports the association constants and free energies of complexation of alkali metal and ammonium picrates by cryptahemispherands **1-3**, diazahemispherand **4**, and cryptands **9-11** at 25 °C in $CDCl_3$ saturated with D_2O. The values obtained are compared with those reported for the spherands in the same

(1) We gratefully acknowledge support of this research from the Division of Basic Sciences of the Department of Energy.

(2) Cram, D. J.; Ho, S. P.; Knobler, C. B.; Maverick, E.; Trueblood, K. N. *J. Am. Chem. Soc.*, preceding paper in this issue.

(3) Cram, D. J.; Kaneda, T.; Helgeson, R. C.; Brown, S. B.; Knobler, C. B.; Maverick, E.; Trueblood, K. N. *J. Am. Chem. Soc.* **1985**, *107*, 3645-3657.

(4) Cram, D. J.; Lein, G. M. *J. Am. Chem. Soc.* **1985**, *107*, 3657-3668.

(5) Lein, G. M.; Cram, D. J. *J. Am. Chem. Soc.* **1985**, *107*, 448-455.

(6) Dietrich, B.; Lehn, J.-M.; Sauvage, J. P.; Blanzat, J. *Tetrahedron* **1973**, *29*, 1629-1645.

(7) Lehn, J.-M. *Struct. Bonding (Berlin)* **1973**, *16*, 1-69.

(8) Graf, E.; Kintzinger, J. P.; Lehn, J.-M.; Le Moigne, J. *J. Am. Chem. Soc.* **1982**, *104*, 1672-1678.

(9) Pedersen, C. J. *Synthetic Multidentate Macrocyclic Compounds*; Izatt, R. M.; Christensen, J. J., Eds.; Academic Press: New York, 1978; pp 1-52.

(10) Artz, S. P.; Cram, D. J. *J. Am. Chem. Soc.* **1984**, *106*, 2160-2170.

0002-7863/86/1508-2998$01.50/0

Chart I

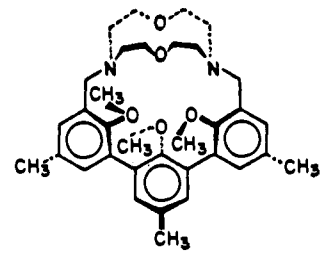

1

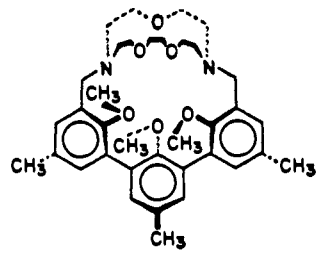

2

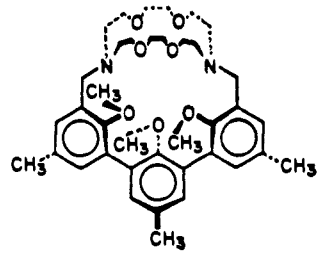

3

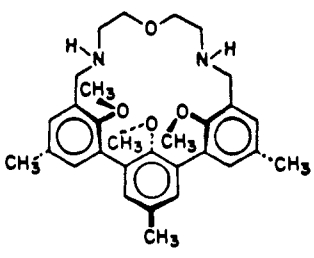

4

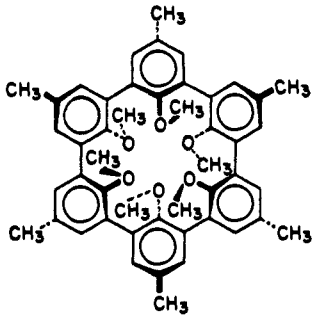

5

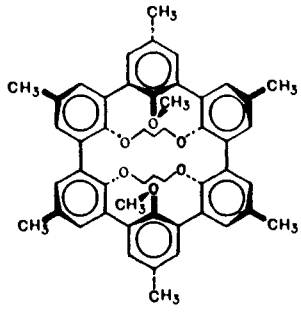

6

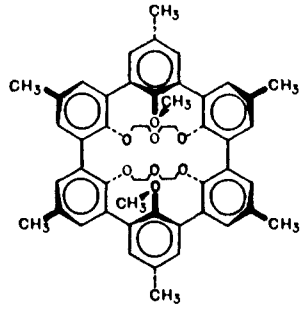

7

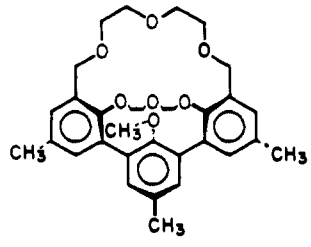

8

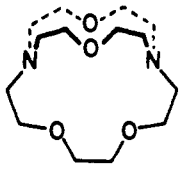

9

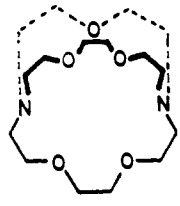

10

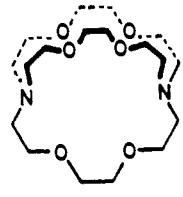

11

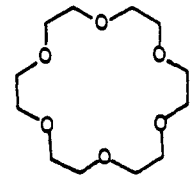

12

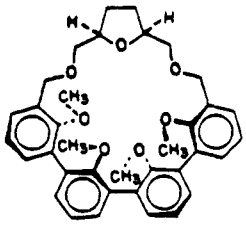

13

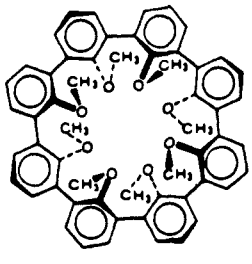

14

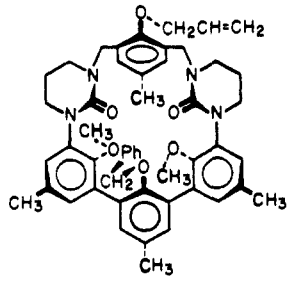

15

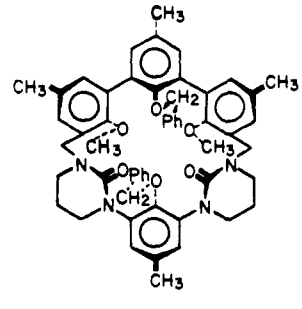

16

medium. The results obtained for the cryptands in this medium are then compared with those obtained by other investigators in other solvents.[7,11,12] The objectives of this research are the following: (1) to determine the relationships between host and guest structures and binding free energies; (2) to probe the limits of ion specificity that can be designed into hosts; and (3) to assess how solvent structure affects binding.

Results

The association constants (K_a, M^{-1}) and free energies of complexation ($-\Delta G°$, kcal mol^{-1}) of the cryptands and cryptahemispherands were obtained through equilibration experiments. Extraction techniques[13] could not be applied to these classes of hosts because of their basicity, the water solubility of their complexes and salts, and their high association constants.[14] The equilibration experiments were conducted at 25 °C in $CDCl_3$ saturated with D_2O. They involved measuring by ^1H NMR techniques the positions of equilibria between two complexes, one

(11) Lehn, J.-M.; Sauvage, J. P. *J. Am. Chem. Soc.* **1975**, *97*, 6700–6707.
(12) Cox, B. G.; Garcia-Rosas, J.; Schneider, H. *J. Am. Chem. Soc.* **1981**, *103*, 1384–1389.

(13) Helgeson, R. C.; Weisman, G. R.; Toner, J. L.; Tarnowski, T. L.; Chao, Y.; Mayer, J. M.; Cram, D. J. *J. Am. Chem. Soc.* **1979**, *101*, 4928–4941.
(14) Keana, Cuomo, Lex, and Seyedrezai (Keana, J. F. W.; Cuomo, J.; Lex, L.; Seyedrezai, S. E. *J. Org. Chem.* **1983**, *48*, 2647–2654) applied the picrate extraction technique to determining the association constants for two cryptands binding Na^+ and K^+. These authors reported $-\Delta G°$ values of ~8–9 kcal mol^{-1}, much lower than ours. Our attempts to apply several modifications of the picrate extraction technique to either the cryptands or the cryptahemispherands failed.

Table I. Association Constants and Free Energies of Complexation of Cryptands with Various Picrate Salts at 25 °C in $CDCl_3$ Saturated with D_2O

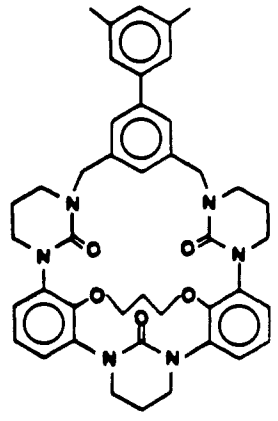

17

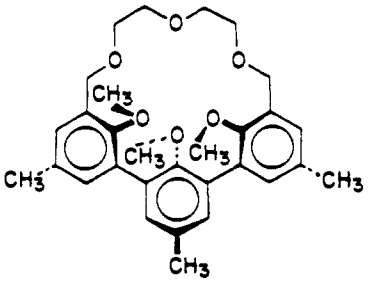

18

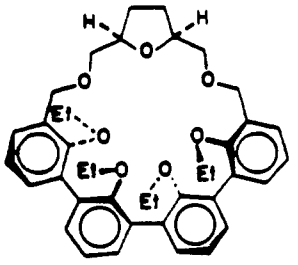

19

host cryptnd	guest ion	no. of runs	K_a (M^{-1})	$-\Delta G°$ (kcal mol^{-1}) $CDCl_3$–D_2O	$-\Delta G°$ (kcal mol^{-1}) CH_3OH–H_2O[a]
[2.1.1], 9[b]	Li^+	7	1.49×10^{12}	16.6	10.3
[2.2.1], **10**[c]	Li^+		2.16×10^{7}	10.0	5.7
[2.2.1], **10**	Na^+	3	9.57×10^{12}	17.7	12.1
[2.2.1], **10**	K^+	2	1.66×10^{11}	15.3	10.2
[2.2.1], **10**	Rb^+	3	2.06×10^{9}	12.7	7.9
[2.2.2], **11**	Na^+	2	3.64×10^{10}	14.4	9.8
[2.2.2], **11**	K^+	3	1.59×10^{13}	18.0	13.3
[2.2.2], **11**	Rb^+	3	2.09×10^{12}	16.8	11.5
[2.2.2], **11**	Cs^+	2	3.58×10^{7}	10.3	4.8
[2.2.2], **11**	NH_4^+	2	4.11×10^{12}	17.2	

[a] Data taken from ref 11. [b] Data taken from ref 4. [c] Estimated, see text.

whose K_a was known and the other whose K_a was being determined. Reference hosts **6–8** and **12–16** were available from prior work. Their K_a values for binding a variety of guests in the same medium had been determined in previous studies.[4,5,15,16] Two methods of equilibration are outlined here. The Experimental section provides the details and the equations involved.

In method A, the picrate salt complex of cryptand **10** or **11** was equilibrated with a host of similar but known K_a value and suitable ^1H NMR spectrum. Hosts **8**[5] and **13–16**[10,16,17] possessed the desired properties. The ^1H NMR signals for the free and complexed forms of the reference host were distinguished, as were the peaks for the picrate protons (~8.8 ppm). Equilibrations took hours, so no difficulties were encountered in measuring initial concentrations. A similar method had previously been applied for determining the K_a and $-\Delta G°$ values for cryptand **9** complexing LiPic.[4] Equilibration experiments that involved **10**·LiPic and reference compounds **13**[10] and **17**[18] indicated only that the $-\Delta G°$ value for **10** lay between 8.9 and 13.6 kcal mol^{-1}. We estimate the value to be 10 kcal mol^{-1} by extrapolation of the linear relationship between $-\Delta G°$ values obtained in $CDCl_3$–D_2O and CH_3OH–H_2O discussed in a future section. Table I records the results.

The K_a and $-\Delta G°$ values of cryptahemispherands **1** and **3** and of diazahemispherand **4** were also determined by method A, except that the cryptand complexes were used as the reference compounds, and the data of Table I were used for the reference K_a and $-\Delta G°$ values. The equilibration of **2** with its diastereomer by ring inversion[2] prevented its determination by exactly the same technique. Accordingly, complexes **2**·LiPic, **2**·NaPic, and **2**·KPic[2] were prepared and equilibrated with free cryptand **11** or spherands **6** or **7** of known K_a values.[4] Table II records the results.

Method B was used to determine the K_a and $-\Delta G°$ values for cryptahemispherand **3** binding CsPic and for **2** binding RbPic,

Table II. Association Constants and Free Energies of Complexation of Cryptahemispherands and Diazahemispherand **4** with Picrate Salts at 25 °C in $CDCl_3$ Saturated with D_2O

host	guest	method	no. of runs	K_a (M^{-1})	$-\Delta G°$ (kcal mol^{-1})
1	Li^+	A	3	6.13×10^{13}	18.8
1	Na^+	A	3	1.28×10^{15}	20.6
1	K^+	A	3	1.00×10^{11}	15.0
1	Rb^+	A	3	5.67×10^{9}	13.3
1	Cs^+	A	1	4.24×10^{7}	10.4
2	Li^+	A	1	6.14×10^{9}	13.4
2	Na^+	A	1	2.59×10^{15}	21.0
2[a]	K^+	A	1	$>3.71 \times 10^{14}$	>19.9
2	Rb^+	B	1	9.18×10^{14}	20.4
2	Cs^+	B	1	1.02×10^{12}	16.4
2	NH_4^+	B	1	4.22×10^{13}	18.6
3[b]	Li^+	A	2	1.82×10^{7}	9.9
3	Na^+	A	3	7.95×10^{9}	13.5
3	K^+	A	3	8.59×10^{13}	19.0
3	Rb^+	A	3	7.72×10^{14}	20.3
3	Cs^+	B	2	8.21×10^{15}	21.7
3	NH_4^+	A	2	6.52×10^{14}	20.2
4[c]	Li^+	A	1	$<8.73 \times 10^{4}$	<6.7
4	Na^+	A	1	3.10×10^{8}	11.6
4[c]	K^+	A	1	$<4.78 \times 10^{8}$	<11.8
4[c]	Rb^+	A	1	$<1.14 \times 10^{7}$	<9.6
4[c]	Cs^+	A	1	$<1.73 \times 10^{5}$	<7.1

[a] Only minimum values for K_a and $-\Delta G°$ could be obtained because of partial overlap of proton signals in the ^1H NMR spectra of the free and complexed hosts. [b] The K_a and $-\Delta G°$ values are based on an approximate value for [2.2.1]cryptand binding LiPic. [c] The K_a and $-\Delta G°$ values are upper limits only because the reference cryptand values were too high to get these complexes of **4** on scale.

(15) Beresford, G. D.; Stoddart, J. F. *Tetrahedron Lett.* **1980**, *21*, 867–870.
(16) Cram, D. J.; Dicker, I. B.; Lauer, M.; Knobler, C. B.; Trueblood, K. N. *J. Am. Chem. Soc.* **1984**, *106*, 7150–7167.
(17) Host **14** has been synthesized and fully characterized, and its K_a and $-\Delta G°$ values have been determined by the picrate extraction method. (Cram, D. J.; Carmack, R., unpublished work).
(18) Host **17** has been synthesized and fully characterized, and its K_a and $-\Delta G°$ values have been determined by the picrate extraction method (Cram, D. J.; Doxsee, K. M., unpublished work).

CsPic, and NH_4Pic. Complex **3**·NH_4Pic was equilibrated with CsPic solubilized by 18-crown-6 (**12**). The K_a value for **3** complexing CsPic was calculated from the integrals of the ^1H NMR spectra, the known K_a values for **12** complexing NH_4Pic and CsPic, and the already determined value (method A) of K_a for **3** complexing NH_4Pic (see Experimental Section). Similarly, **2**·LiPic was equilibrated with RbPic, CsPic, and NH_4Pic solubilized by **12**.[15] The resultant K_a and $-\Delta G°$ values for **2** complexing RbPic, CsPic, and NH_4Pic were calculated. Table II records the results.

Free cryptahemispherand **2** exists in solution as the dominant diastereomeric isomer by a factor of about five over the subordinate isomer in which the two methoxy groups and the shorter of the two $(CH_2OCH_2)_m$ bridges are syn to one another. The two free hosts equilibrate very rapidly on the human but slowly on the ^1H NMR time scale at ambient temperature. When the mixture was submitted to complexation conditions, only complexes of isomer **2** were detectable by ^1H NMR. The crystal structure of **2**·KSCN confirmed the structural assignment based on ^1H NMR spectral comparisons.[2]

Discussion

Structures and Binding Strengths of the Cryptahemispherands. The smallest of the cryptahemispherands, host **1**, possesses seven potential binding sites, all of which are used in the crystal structure of **1**·Na^+.[2] The $-\Delta G°$ values (kcal mol^{-1}, Table II) peak at 20.6 kcal mol^{-1} with Na^+ as guest and are the lowest at 10.4 for Cs^+, thus providing a range of 10.2 kcal mol^{-1} for the five alkali metal ions. The five ions are bound in the following decreasing order of $-\Delta G°$ values: $Na^+ > Li^+ > K^+ > Rb^+ > Cs^+$. Thus lithium appears too small, and K^+, Rb^+, and Cs^+ are too large for inclusion in the cavity without paying the costs of straining the host. It would be interesting to calculate these strain energies, something we do not plan to do. Comparisons of CPK molecular model complexes with spheres of standard ionic dimensions[19] suggest that the most strain-free cavity of **1** would have to contract somewhat if all seven heteroatoms contacted Li^+ and would have to expand increasingly to accommodate K^+, Rb^+, and Cs^+.

The medium-sized cryptahemispherand **2** possesses eight potential binding sites, all of which are used in the crystal structure of **2**·K^+.[2] The $-\Delta G°$ values (kcal mol^{-1}, Table II) peak with Na^+ or possibly with K^+ as guest at 21.0 and >19.9 kcal mol^{-1}, respectively. The lowest value involves Li^+, with a $-\Delta G°$ value of 13.4, to provide a total range of 7.6 or more kcal mol^{-1} for the alkali metal and ammonium ions. The ions are bound in the following decreasing order of $-\Delta G°$ values: Na^+ or $K^+ > Rb^+ > NH_4^+ > Cs^+ > Li^+$. Thus lithium appears much too small, and Cs^+ appears too large to be complementary to the least-strained cavity. Molecular model examinations suggest that K^+ is the most complementary to the least-strained cavity, Rb^+, NH_4^+, and Na^+ are next, and Li^+ is the least, being unable to simultaneously contact more than five ligating heteroatoms.

The largest cryptahemispherand **3** possesses nine potential binding sites, all of which are used in the crystal structures of **3**·Cs^+ and **3**·K^+, but only five are used in that of **3**·Na^+.[2] Interestingly, the conformational organizations of the hosts are similar in all three crystal structures; however, those of **3**·Na^+ and **3**·Cs^+ are more similar to each other than to that of **3**·K^+. Thus **3** had adapted less to Na^+ than to K^+ as guest, but as a result, four ligating sites are not used in primary binding in **3**·Na^+. The $-\Delta G°$ values for **3** peak with Cs^+ as guest at 21.7 kcal mol^{-1} and are the lowest for Li^+ at 9.9 kcal mol^{-1}, providing a range of 11.8 kcal mol^{-1}. The ions are bound in the following decreasing order of $-\Delta G°$ values: $Cs^+ > Rb^+ \sim NH_4^+ > K^+ > Na^+ > Li^+$. Molecular model examinations suggest that Cs^+, Rb^+, and NH_4^+ ions should be the most complementary to the least strained cavity, K^+ the next, and Na^+ and Li^+ the least, the latter being unable to reach more than five ligating heteroatoms simultaneously. In molecular models, Li^+ and 1 molecule of water nicely fit into the cavity of 3 without strain. However in models, Na^+ and 1 molecule of water fit into the cavity of **3** only by straining the support structure. There is no water in the crystal structure of **3**·Na^+. The ^1H NMR spectra of **3**·Li^+ and **3**·Na^+ in solution provide no evidence of encapsulated water. Were it there, both it and the metal ion would have to be moving about in the cavity at a rate rapid on the ^1H NMR time scale to provide the complexes the equivalent of a mirror plane.

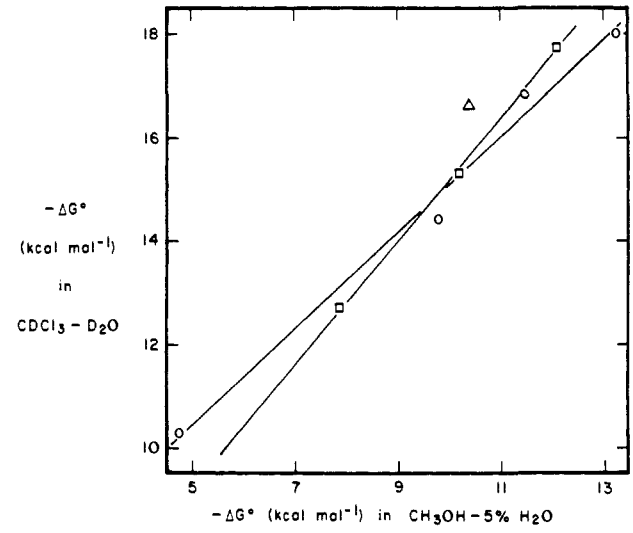

Figure 1. Free energies of complexation of alkali metal ions by cryptands in $CDCl_3$ saturated with D_2O vs. 95% CH_3OH–5% H_2O: △, [2.1.1]-cryptand binds Li^+; □, [2.2.1]cryptand binds Li^+, Na^+, and K^+; ○, [2.2.2]cryptand binds Na^+, K^+, Rb^+, and Cs^+.

Cryptand Binding Strengths and Solvent Effects. The cryptands exhibit lower binding strengths and ranges than the cryptahemispherands. The highest $-\Delta G°$ values obtained in $CDCl_3$–D_2O for the cryptands were for [2.2.2]cryptand **11** binding K^+ with 18.0 kcal mol^{-1} and for [2.2.1]cryptand **10** binding Na^+ with 17.7 kcal mol^{-1}. These values are 3–4 kcal mol^{-1} lower than the peak binding observed for the cryptahemispherands. The range of values for these three cryptands is 8 kcal mol^{-1}, whereas it is ~12 kcal mol^{-1} for the three cryptahemispherands.

Cox et al.[12] have shown that the cryptand complexes are the most stable in aprotic, nonpolar solvents and are the least stable in aqueous or polar solvents. Ion-solvent interactions are relatively weak in aprotic, nonpolar solvents, which allows the interactions of the positively charged ions with the electron-rich ligands to be fully expressed. The $-\Delta G°$ values (kcal mol^{-1}) for the cryptands binding the alkali metal ions in 95% CH_3OH–5% H_2O (v)[11] are listed in Table I. When the $-\Delta G°$ values of the cryptand complexes in $CDCl_3$–D_2O were plotted against those in CH_3OH–H_2O, the straight lines of Figure 1 were obtained to give correlation coefficients of about 0.99. This correlation proved useful in providing an estimate of the $-\Delta G°$ value for [2.2.1]cryptand **10** binding LiPic of 10 kcal mol^{-1} (see former section).

The correlation extends more roughly to all data points available (eight) covering the three cryptands binding all five of the alkali metal ions. Thus the $-\Delta G°$ values in CH_3OH–H_2O are 5.2 ± 0.4 kcal mol^{-1} lower than those in $CDCl_3$–D_2O. This correlation indicates that ion selectivity for the cryptands should not vary widely in passing from CH_3OH–H_2O to $CDCl_3$–D_2O. These correlations probably reflect the cancellation of a large number of effects. Similar trends are visible in the data of Cox for the cryptands binding the alkali metal ions in nine different solvents of widely differing character.[12] Of the nine solvents, $CH_2(CH_2O)_2CO$ and CH_3CN are the most similar in their $-\Delta G°$ values to $CDCl_3$–D_2O. For all host–guest combinations, the binding strength in $CDCl_3$–D_2O is greater than in any other medium.

Ion Selectivity and Host Structure. The importance of Li^+, Na^+, and K^+ to biological processes, the susceptibility of Rb^+ and Cs^+ to neutron activation, the possible use of $^6Li^+$ as a fusion fuel, and the evolution of FABMS have combined to generate increasing interest in hosts that differentially bind these ions. High selectivity factors among Li^+, Na^+, and K^+ are particularly important to

(19) Pauling, L. C. *Nature of the Chemical Bond*, 2nd ed.; Cornell: Ithaca, New York, 1940, pp 189 and 350.

analytical methods for measuring concentrations of these ions in serum and urine. In this section we compare the selectivity factors as measured by relative values of K_a in $CDCl_3$–D_2O for various pairs of host–guest partners. The distribution constants between D_2O and $CDCl_3$–D_2O for the five alkali metal ion picrate salts differ from one another by factors of less than two for cations neighboring one another in the periodic table. The largest factor involving *any two ions* is only 3.8.[20] Thus K_a^A/K_a^B ratios provide a reasonable measure of ion selectivity in extraction as well as in homogeneous media. Table III compares the K_a^A/K_a^B values of the cryptahemispherands, cryptands, spherands, and two hemispherands (**8** and **19**[10]) for pairs of neighboring ions.

Of the hosts listed, only spherands **5** and **6** show lithium over sodium ion selectivity (factors of >600 and 360, respectively). Impressive selectivities of sodium over lithium ion are exhibited by cryptahemispherand **2** (420 000), cryptand **10** (440 000), and bridged hemispherand **8** (9 500). The highest selectivities found in Table III involve the factors of $>10^{10}$, $>10^5$, and $>10^9$ observed for the spherands **5**–**7** binding sodium over potassium ion. However, cryptahemispherand **1** provides the substantial selectivity factor of 13 000 for sodium over potassium ion. Cryptahemispherand **3** shows the highest potassium over sodium ion selectivity factor of 11 000, followed by hemispherand **19** with 2 000, and finally by cryptand **11** with 440. Cryptand **10** shows the highest potassium over rubidium ion factor of 81, followed by bridged hemispherand **8** with a factor of 34. Cryptand **11** provides the large rubidium over cesium ion factor of 58 000, followed by cryptahemispherand **2** with 900, and **1** with 134. Of the hosts listed, the only one that binds cesium better than rubidium ion is cryptahemispherand **3** (factor of ~11).

An interesting question arises about the relationship between peak binding and selectivity. For hosts **1**, **2**, **7**, and **10**, the largest selectivities between neighboring ions involves one ion that exhibits peak binding. However, with hosts **3**, **5**, **6**, **8**, **11**, and **19**, peak binding does not involve either of the ions that produce maximum selectivity. In other words, the largest differences in complementarity do not necessarily involve the most complementary relationships between complexing partners. Cryptahemispherand **3** best illustrates this point. Peak binding occurs with Cs^+ with $-\Delta G° = 21.7$ kcal mol^{-1}, but the largest selectivity occurs between K^+ ($-\Delta G° = 19.0$) and Na^+ ($-\Delta G° = 13.5$). Thus to maximize selectivity, hosts must be designed both to maximize and minimize complementarity.

Table IV identifies the most complementary host–guest relationships for the three cryptahemispherands and two spherands of this study and relates the highest selectivity to forces that destabilize the less stable complex of the pair. These forces roughly collect into categories of cavity-expansion strain and cavity-contraction strain, which produce a misalignment and placement of ligands with respect to guest ion. The former represents the deformations of normal bond angles and lengths and atom compressions growing out of lengthening the molecular modules to accommodate a misfitting guest. The latter represents the deformations and compressions associated with shortening the molecular modules. Of the five examples of selectivity cited in Table IV, two grow out of expansion strain and three out of contraction strain.

Relationships between Preorganization of Hosts, Binding, and Selectivity. The results of this paper coupled with those obtained previously in this series provide the following order when classes of hosts are arranged according to the $-\Delta G°$ with which they bind their most complementary guests: spherands > cryptahemispherands > cryptands > hemispherands > chorands > podands > solvent. This same order is less rigidly followed when maximum ion selectivity is applied to the host classes in the form of $-\Delta(\Delta G°)_B^A$ values: spherands > cryptahemispherands ~ cryptands > hemispherands > chorands > podands. Table V provides illustrations of these generalizations in which standard lipophilic chorand **20**[13] and podand **21**[4] are included.

(20) Koenig, K. E.; Lein, G. M.; Stückler, P.; Kaneda, T.; Cram, D. J. *J. Am. Chem. Soc.* **1979**, *101*, 3553–3566.

Both crystal structure determinations and CPK molecular model examinations indicate that the above order of host classes correspond to the order of preorganization of the ligating sites by their support structure.[2,3] The conformations of the oxygens in the spherands and in the anisyl modules of the cryptahemispherands and hemispherands are fixed during synthesis to maximize capsular binding of spherical guests and to shield their binding electron pairs from solvation. The $CH_2N(CH_2)_2$ and $(CH_2OCH_2)_m$ modules are conformationally mobile, their unshared electron pairs are more exposed to solvation, and their methylene groups can turn inward to fill the cavity. Substitution of a trisanisyl for a $(CH_2OCH_2)_m$ bridge of a cryptand as in the cryptahemispherands provides three preorganized, nonsolvated oxygens to the system, thereby increasing its binding power.

Diazahemispherand 4. Monocyclic host **4** was synthesized for comparisons with its oxygen analogue, hemispherand **18**, and its cryptahemispherand relative **1**. The only K_a and $-\Delta G°$ values that were "on scale" involved **4** binding NaPic. Upper limits were placed on $-\Delta G°$ values for the other guests (Table II). The $-\Delta G°$ value of 11.6 kcal mol^{-1} for **4** binding NaPic is close to the 12.2 kcal mol^{-1} observed for **18** binding NaPic but is far less than the 20.6 kcal mol^{-1} obtained for **1** binding the same guest. The dramatic increase in binding power of **1** over **4** provides another example of the effect of decreasing the number of degrees of rotational freedom of the $(CH_2OCH_2)_m$ and $CH_2N(CH_2)_2$ modules by introduction of an additional bridge to the macrocycle. Because of space limitations of the cavity, only two methylenes at the most can turn inward to fill the cavities of **1**, **4**, or **18**. Addition of one more bridge as in **1** in effect provides one more *preorganized binding site* and many more outward-turned methylenes, which shield the unshared electron pairs from solvation. The upper limits placed on the $-\Delta G°$ values for **4** binding the other picrate salts indicate the host to be unremarkable in its binding pattern.

Experimental Section

Potassium(1+) 4,7,13,16,21-Pentaoxa-1,10-diazabicyclo[8.8.5]tricosane Picrate (10·KPic). Complexes **9**·LiPic, **10**·NaPic, and **11**·KPic have already been reported.[4] The synthesis by procedure A is illustrated with that of **10**·KPic. Cryptand **10** (280 mg) in 15 mL of methanol was stirred 12 h with 329 mg of KPic. The solvent was evaporated, and the residue was triturated with CH_2Cl_2. The mixture was filtered to remove the excess salt, the filtrate was evaporated, and the resulting complex was crystallized from EtOAc and hexane to give an essentially quantitative yield of **10**·KPic, mp 124 °C: ^{1}H NMR ($CDCl_3$) δ 2.45–2.61, 2.86–2.99 (m, 12 H, NCH_2), 3.40–3.66 (m, 20 H, OCH_2), 8.87 (s, 2 H, ArH). Anal. Calcd for $C_{22}H_{34}N_5O_{10}K$: C and H.

Lithium(1+) 4,7,13,16,21-Pentaoxa-1,10-diazabicyclo[8.8.5]tricosane Picrate (10·LiPic). Application of procedure A to **10** and LiPic gave **10**·LiPic, mp 44–46 °C: ^{1}H NMR ($CDCl_3$) δ 2.68–2.78 (m, 12 H, NCH_2), 3.48–3.70 (m, 20 H, OCH_2), 8.81 (s, 2 H, ArH). Anal. Calcd for $C_{22}H_{34}N_5O_{12}Li$: C and H.

Rubidium(1+) 4,7,13,16,21-Pentaoxa-1,10-diazabicyclo[8.8.5]tricosane Picrate (10·RbPic). Application of procedure A to **10** and RbPic gave **10**·RbPic crystallized from CH_2Cl_2 and ether, mp 117 °C: ^{1}H NMR ($CDCl_3$) δ 2.43–2.63, 2.82–2.95 (m, 12 H, NCH_2), 3.41–3.73 (m, 20 H, OCH_2), 8.86 (s, 2 H, ArH). Anal. Calcd for $C_{22}H_{34}N_5O_{12}Rb$: C and H.

Sodium(1+) 4,7,13,16,21,24-Hexaoxa-1,10-diazabicyclo[8.8.8]hexacosane Picrate (11·NaPic). Application of procedure A to **11** and NaPic gave **11**·NaPic crystallized from THF and hexane, mp 129 °C: ^{1}H NMR ($CDCl_3$) δ 2.65 (t, 12 H, J = 5.4 Hz, NCH_2), 3.58 (t, 12 H, J = 5.4 Hz, OCH_2), 3.62 (s, 12 H, OCH_2), 8.82 (s, 2 H, ArH). Anal. Calcd for $C_{24}H_{38}N_5O_{13}Na$: C and H.

Rubidium(1+) 4,7,13,16,21,24-Hexaoxa-1,10-diazabicyclo[8.8.8]hexacosane Picrate (11·RbPic). Application of procedure A to **11** and RbPic gave **11**·RbPic crystallized from THF and hexane, mp 126–127 °C: ^{1}H NMR ($CDCl_3$), δ 2.51 (t, 12 H, J = 4.3 Hz, NCH_2), 3.48 (t, 12 H, J = 4.3 Hz, OCH_2), 3.57 (s, 12 H, OCH_2), 8.81 (s, 2 H, ArH). Anal. Calcd for $C_{24}H_{38}N_5O_{13}Rb$: C, H, and N.

Cesium(1+) 4,7,13,16,21,24-Hexaoxa-1,10-diazabicyclo[8.8.8]hexacosane Picrate (11·CsPic). Application of procedure A to **11** and CsPic gave **11**·CsPic crystallized from CH_2Cl_2 and EtOAc, mp 88–90 °C: ^{1}H NMR ($CDCl_3$) δ 2.50 (t, 12 H, J = 4.4 Hz, NCH_2), 3.46 (t, 12 H, J = 4.4 Hz, OCH_2), 3.56 (s, 12 H, OCH_2), 8.76 (s, 2 H, ArH). Anal. Calcd for $C_{24}H_{38}N_5O_{13}Cs$: C and H.

Table III. Selectivities in Complexation by Cryptahemispherands, Cryptands, Spherands, and Hemispherands of Alkali Metal Ion Picrates at 25 °C in $CDCl_3$ Saturated with D_2O as Measured by K_a^A/K_a^B Values

host	K_a^{Li}/K_a^{Na}	K_a^{Na}/K_a^{Li}	K_a^{Na}/K_a^{K}	K_a^{K}/K_a^{Na}	K_a^{K}/K_a^{Rb}	K_a^{Rb}/K_a^{Cs}
1		21	13 000		18	134
2		420 000	<6			900
3		440		11 000	0.11	0.094
10		440 000	58		81	
11				440	8	58 000
5[a]	>600		$>10^{10}$			
6[a]	360		$>10^{5}$			
7[a]		125	$>10^{9}$			
8		9 500		7	34	34
19[b]		3		2 000	1	5

[a] Reference 4. [b] Reference 10.

Table IV. Host–Guest Complementarity and Selectivity Associated with Noncomplementarity

most complmntry			highst selctvty		cavty of less stable complx straind by
host	ion	$-\Delta G°$ (kcal mol^{-1})	ions	K_a^A/K_a^B	
1	Na^+	20.6	Na^+/K^+	13 000	expnsn
2[a]	Na^+	21.0	Na^+/Li^+	420 000	contrctn
3	Cs^+	21.7	K^+/Na^+	11 000	contrctn
10	Na^+	17.7	Na^+/Li^+	440 000	contrctn
11	K^+	18.0	Rb^+/Cs^+	58 000	expnsn

[a] K^+ might be comparably or better bound.

Ammonium(1+) 4,7,13,16,21,24-Hexaoxa-1,10-diazabicyclo[8.8.8]-hexacosane Picrate (11·NH_4Pic). Application of procedure A to **11** and NH_4Pic gave **11**·NH_4Pic crystallized from CH_2Cl_2 and EtOAc, mp 140 °C: ^{1}H NMR ($CDCl_3$) δ 2.54 (t, 12 H, J = 4.9 Hz, NCH_2), 3.54 (t, 12 H, J = 4.9 Hz, OCH_2), 3.62 (s, 12 H, OCH_2), 6.90 (t, 4 H, J = 51.8 Hz, NH_4), 8.83 (s, 2 H, ArH). Anal. Calcd for $C_{24}H_{42}N_6O_{13}$: C and H.

Determination of Association Constants by Equilibration Experiments Involving Two Hosts and One Guest. Method A. In these experiments the host or complex whose K_a was being determined was mixed in $CDCl_3$ (saturated with D_2O) with a reference complex or host whose K_a value had already been determined. The redistribution of the guest (G) between AG and BG was followed to equilibrium through changes in the ^{1}H NMR spectrum of the solution over many hours. The equilibria involved are described by eq 1–2, which define K_a^A and K_a^B. The ^{1}H

$$A + G \underset{}{\overset{K_a^A}{\rightleftharpoons}} AG \qquad B + G \overset{Ka^B}{\rightleftharpoons} BG \tag{1}$$

$$K_a^B/K_a^A = [BG]_e[A]_e/[AG]_e[B]_e \tag{2}$$

NMR signals for the free and complexed forms of B were distinguished and integratable, as were the peaks for the picrate protons around 8.8 ppm, which provided concentrations of the initial complex used. The picrate protons required a longer than normal relaxation period. The use of a pulse width of 1.8 units and a relaxation delay of 5 s provided a correct integral for these protons. The subscripts e and i to the concentration terms in the equations refer to equilibrium and initial conditions, respectively.

The values for the ratios of concentration terms in eq 2 were calculated as follows. The ratios of $[AG]_i/[B]_i$ and $[BG]_e/[B]_i$ were obtained from the integrals of the signals for $[AG]_i$ (the picrate peak), [B], and [BG]. These values and eq 3–5 provided the ratios $[BG]_e/[AG]_e$ and $[A]_e/[B]_e$

$$[AG]_e/[B]_i = [AG]_i/[B]_i - [BG]_e/[B]_i \tag{3}$$

$$[A]_e/[B]_i = [BG]_e/[B]_i \tag{4}$$

$$[B]_e/[B]_i = 1 - [BG]_e/[B]_i \tag{5}$$

needed in eq 2 to calculate K_a^B/K_a^A. Given the latter values and one of the two K_a values, the other was calculated. Table VI lists the following: the hosts or complexes whose association constants were being studied; the reference hosts or complexes whose association constants had been determined; the values of the measured integral ratios; the calculated values for K_a^B/K_a^A; the desired value of K_a; and the derived $-\Delta G°$ value for the cryptand, cryptahemispherand, or diazahemispherand.

The NMR tubes were washed with acetone, deionized water, and ethanol and dried in the oven. Syringes were washed with acetone, deionized water, and methylene chloride and air-dried overnight before use. Volumetric flasks were washed with chromerge, ammonium hydroxide, and deionized water and dried in the oven. Deuteriochloroform with a minimum isotopic purity of 99.96% was filtered over activity I basic alumina and then saturated with D_2O. Stock solutions of cryptahemispherands, cryptand complexes, and other hosts were prepared by dissolving the appropriate amounts of compound in $CDCl_3$–D_2O to give 3.4 mM solutions. Aliquots (250 μL) of free host and complexed host were mixed in an NMR tube, together with 100 μL of a 0.042 M solution of Et_3N in $CDCl_3$–D_2O. The amine was added in excess to neutralize any acid liberated by the solvent with time. The NMR tubes were sealed with Teflon tape and kept in the dark at 25 °C. The competition between the two hosts was followed over a period of 5–10 days to ensure that equilibrium had been reached. Where necessary, more of one or the other stock solution was added to the NMR tube. Protons of the free and complexed forms of one of the hosts were integrated.

Determination of Association Constants by Equilibration Experiments between Two Different Complexes To Give Four Complexes. Method B.

Table V. Relationships between Degree of Preorganization of Host Classes, Their Binding Power, and Their Ion Selectivity

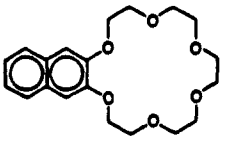

20

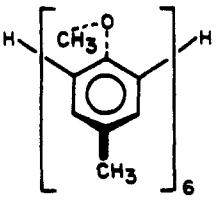

21

host class	host	guest	$-\Delta G°$ (kcal mol^{-1})	guests A	guests B	$-\Delta(\Delta G°)_B^A$ (kcal mol^{-1})
spherand	**5**	Li^+	>23	Na^+	K^+	>13
cryptahemispherand	**3**	Cs^+	21.7	K^+	Na^+	5.5
cryptand	**11**	K^+	18.0	Rb^+	Cs^+	6.5
hemisherand	**19**	K^+	11.6	K^+	Na^+	4.5
chorand	**20**	K^+	10.8	K^+	Na^+	2.5
podand	**21**	all	<6	too low to measure		

Table VI. Parameters Used to Calculate Association Constants (K_a) and Free Energies of Complexation by Hosts of Alkali Metal or Ammonium Picrates at 25 °C in $CDCl_3$ Saturated with D_2O Determined by Method A

hosts or complexes studied	reference struct	$-\Delta G°$ [a]	$[AG]_i/[B]_i$	$[BG]_e/[B]_i$	K_a^B/K_a^A	K_a [b] (M^{-1})	$-\Delta G°$ [a]	$-\Delta G°_{ave}$ [a]
10·NaPic	**15**	16.5	1.302	0.295	0.122	1.03×10^{13}	17.74	
			1.279	0.313	0.147	8.58×10^{12}	17.64	17.7
			1.340	0.279	0.102	1.24×10^{13}	17.85	
10·KPic	**8**	14.0	0.975	0.246	0.110	1.68×10^{11}	15.31	15.3
			0.978	0.257	0.123	1.50×10^{11}	15.24	
10·RbPic	**13**	12.2	1.078	0.415	0.443	2.00×10^{9}	12.68	
			1.091	0.446	0.557	1.59×10^{9}	12.55	12.7
			1.242	0.414	0.353	2.51×10^{9}	12.82	
11·NaPic	**16**	15.9	0.979	0.786	14.96	3.06×10^{10}	14.30	14.4
			0.957	0.753	11.25	4.07×10^{10}	14.47	
11·KPic	**15**	17.1	1.015	0.326	0.229	1.52×10^{13}	17.97	
			0.922	0.338	0.296	1.17×10^{13}	17.82	18.0
			1.077	0.281	0.138	2.52×10^{13}	18.27	
11·RbPic	**15**	14.3	0.786	0.090	0.013	2.36×10^{12}	16.87	
			0.895	0.101	0.014	2.19×10^{12}	16.83	16.8
			0.809	0.097	0.015	2.05×10^{12}	16.79	
11·CsPic	**14**	11.8	0.515	0.494	23.37	1.93×10^{7}	9.93	10.3
			0.889	0.692	7.892	5.71×10^{7}	10.58	
11·NH_4Pic	**15**	14.4	1.12	0.098	0.010	3.64×10^{12}	17.13	17.2
			0.837	0.076	0.008	4.55×10^{12}	17.26	
1	9·LiPic	16.6	0.940	0.831	37.84	5.65×10^{13}	18.75	
			0.941	0.873	36.82	5.50×10^{13}	18.74	18.8
			1.148	0.934	62.06	9.27×10^{13}	19.04	
1	**11**·NaPic	17.7	1.000	0.920	132.25	1.27×10^{15}	20.59	
			1.019	0.942	198.90	1.90×10^{15}	20.83	20.6
			1.156	0.952	92.56	8.86×10^{14}	20.38	
1	**11**·KPic	15.3	2.500	0.600	0.474	7.88×10^{10}	14.86	
			2.393	0.654	0.711	1.18×10^{11}	15.10	15.0
			2.201	0.603	0.574	9.54×10^{10}	14.97	
1	**11**·RbPic	12.7	1.318	0.716	2.999	6.18×10^{9}	13.35	
			1.971	0.822	3.295	6.79×10^{9}	13.41	13.3
			2.930	0.860	2.550	5.25×10^{9}	13.25	
1	**11**·CsPic	10.3	1.360	0.600	1.184	4.24×10^{7}	10.40	10.4
2·LiPic	**6**	16.8	0.843	0.831	341	6.14×10^{9}	13.4	
2·NaPic	**7**	18.7	0.300	0.067	0.020	2.59×10^{15}	21.0	
2·KPic	**11**	18.0	0.082	<0.041	<0.043	$>3.71 \times 10^{14}$	>19.9	
3	**10**·LiPic	10.0 [b]	1.757	0.637	0.998	2.16×10^{7}	10.0	9.9
			1.505	0.557	0.738	1.59×10^{7}	9.82	
3	**11**·NaPic	14.4	1.241	0.349	0.210	7.64×10^{9}	13.48	
			1.162	0.342	0.216	7.85×10^{9}	13.49	13.5
			0.967	0.319	0.231	8.40×10^{9}	13.53	
3	**11**·KPic	18.0	1.235	0.753	4.76	7.56×10^{13}	18.92	
			1.233	0.753	4.78	7.59×10^{13}	18.93	19.0
			1.016	0.743	7.78	1.24×10^{14}	19.21	
3	**11**·RbPic	16.8	0.940	0.913	355	7.43×10^{14}	20.28	
			0.960	0.920	265	5.55×10^{14}	20.10	20.3
			0.740	0.735	503	1.05×10^{15}	20.48	
3	**11**·NH_4Pic	17.2	0.920	0.887	220	9.05×10^{14}	20.40	20.2
			0.890	0.850	117	4.81×10^{14}	20.02	
4	**10**·LiPic	10.0 [b]	0.700	<0.050	<0.004	$<8.73 \times 10^{4}$	<6.7	
4	**11**·NaPic	14.4	0.935	0.002	0.009	3.10×10^{8}	11.6	
4	**11**·KPic	15.3	0.965	<0.050	<0.003	$<4.78 \times 10^{8}$	<11.8	
4	**11**·RbPic	12.7	0.526	<0.050	<0.006	$<1.14 \times 10^{7}$	<9.6	
4	**11**·CsPic	10.3	0.551	<0.050	<0.005	$<1.73 \times 10^{5}$	<7.1	

[a] Kcal mol^{-1}. [b] For **10** and **11** systems studied, K_a^A corresponded to calculated K_a. For study of system **1**, K_a^B corresponded to calculated K_a. For study of complexes of **2**, K_a^A corresponded to calculated K_a. For study of systems **3** and **4**, K_a^B corresponded to calculated K_a. [c] Value estimated by extrapolation in Figure 1.

In these experiments, a host–guest complex of known K_a was dissolved at 25 °C in $CDCl_3$ saturated with D_2O. A second complex was added, whose host was 18-crown-6 **12** and whose guest cation was that whose K_a with the first host was to be measured. The two complexes were allowed to come to equilibrium as described in eq 6, which defines K_e.

$$AB + CD \overset{K_e}{\rightleftharpoons} AD + CB \quad (6)$$

In eq 6, AB is the complex of host A and picrate salt B, whose K_a is known from Table VI; CD is the complex of 18-crown-6 **12** and picrate salt D, whose K_a^{CD} is known;[15] AD is the complex of host A and picrate salt D, whose K_a^{AD} is being determined; CB is the complex of 18-crown-6 **12** and picrate salt B, whose K_a^{CB} is known.[15] Equation 7 relates K_e to the equilibrium concentrations and association constants (K_a) for the four complexes, and eq 8 expresses the desired K_a^{AD} in terms of known or measurable parameters. Equation 9 is eq 7 in which each concentration term is divided by the initial concentration of AB, $[AB]_i$. Equations 10–12 express the terms of eq 9 in obtainable concentration ratios.

$$K_e = [CB]_e[AD]_e/[AB]_e[CD]_e = K_a^{AD}K_a^{CB}/K_a^{AB}K_a^{CD} \quad (7)$$

$$K_a^{AD} = K_a^{AB}K_e(K_a^{CD}/K_a^{CB}) \quad (8)$$

$$K_e = \frac{([CB]_e/[AB]_i)([AD]_e/[AB]_i)}{([AB]_e/[AB]_i)([CD]_e/[AB]_i)} \quad (9)$$

$$[AB]_e/[AB]_i = 1 - ([AD]_e/[AB]_i) \quad (10)$$

$$[CB]_e/[AB]_i = [AD]_e/[AB]_i \quad (11)$$

$$[CD]_e/[AB]_i = ([\text{total pic}]/[AB]_i) - 1 - ([AD]_e/[AB]_i) \quad (12)$$

Table VII. Association Constants and Free Energies of Complexation at 25 °C in $CDCl_3$ Saturated with D_2O Determined by Equilibration Experiments between Two Host–Guest Picrate Complexes Whose Cationic Partners Disproportionate

picrate complexes								
	reference							
studied AD	AB	CD	$[CD]_i/[AB]_i$	$[AD]_e/[AB]_i$	K_e	K_a^{CD}/K_a^{CB} [b]	K_a^{AD} [a] (M^{-1})	$-\Delta G°$ (kcal mol^{-1})
2·Rb^+	**2**·Li^+	**12**·Rb^+	2.703	0.810	1.82	8.20×10^4	9.18×10^{14}	20.4
2·Cs^+	**2**·Li^+	**12**·Cs^+	3.969	0.200	0.013	1.28×10^4	1.02×10^{12}	16.4
2·NH_4^+	**2**·Li^+	**12**·NH_4^+	1.829	0.679	1.25	5.50×10^3	4.22×10^{13}	18.6
3·Cs^+	**3**·NH_4^+	**12**·Cs^+	0.695	0.530	3.62	2.32	5.50×10^{15}	21.5
			0.668	0.562	6.80	2.32	1.03×10^{16}	21.8

[a] The K_a^{AB} values used to calculate these values are taken from Table VI and are as follows: for LiPic binding **2**, $K_a^{AB} = 6.14 \times 10^9$ M^{-1}; for NH_4Pic binding **3**, $K_a^{AB} = 6.53 \times 10^{14}$ M^{-1}. [b] The K_a values for 18-crown-6 binding the various picrate salts at 25 °C in $CDCl_3$ saturated with D_2O are as follows: Li^+, 4.44×10^5 M^{-1}; Rb^+, 3.64×10^{10} M^{-1}; NH_4^+, 2.44×10^9 (ref 15). That for Cs^+ was estimated to be 5.67×10^9 M^{-1} by interpolating a linear plot (similar to Figure 1) of $-\Delta G°$ values for KPic, RbPic, and NH_4Pic binding 18-crown-6 in $CDCl_3$–D_2O at 25 °C, and $-\Delta G°$ values for 18-crown-6 binding the same ions in CH_3OH (De Jong, F.; Reinhoudt, D. N. *Adv. Phys. Org. Chem.* **1980**, *17*, 279–433). These authors reported the K_a values for 18-crown-6 binding Cs^+ in CH_3OH but did not report the K_a for 18-crown-6 binding CsPic in $CDCl_3$–D_2O (ref 15).

Experimentally, stock solutions of the various complexes were prepared and mixed as in method A. The ^1H NMR spectral signals of complexes AB and AD were distinguished and integrated, as were the signals of total picrate ion. These signals were integrated immediately to give $[CD]_i/[AB]_i$ ratios, AB directly, and CD from total pic − AB. The complexes were allowed to equilibrate at 25 °C in the dark. After many hours, the integrals stopped changing, at which time AB, AD, and total pic integrals were taken. These, coupled with the initial integrals, gave $[AB]_e/[AB]_i$ directly, $[AD]_e/[AB]_i$ from eq 10, $[CB]_e/[AB]_i$ from eq 11, and $[CD]_e/[AB]_i$ from eq 12. These values and eq 8 provided K_e values, which coupled with the known values of K_a^{AB}, K_a^{CB}, and K_a^{CD} and eq 8 provided the desired K_a^{AD} values. Table VII identifies the complex AD whose K_a^{AD} is being determined, the reference complexes AB and CD, and lists the values of $[CD]_i/[AB]_i$, $[AD]_e/[AB]_i$, K_e, and K_a^{CD}/K_a^{CB}.

Molecularity in the Equilibria. The equations developed for converting the data of methods A and B into K_a and $-\Delta G°$ values are valid only if the hosts and their complexes are monomeric at 25 °C in $CDCl_3$ saturated with D_2O at concentrations $\approx 10^{-3}$ M. In extensive work in which we applied the picrate salt extraction method to a variety of chorands and hemispherands, we demonstrated the $-\Delta G°$ values obtained at 25 °C in $CDCl_3$ saturated with water were independent (within error) of initial concentrations of host and guest ranging from 0.015 to 0.001 M.[5,13] Many different experimentalists obtained $-\Delta G°$ values within 0.2 kcal mol^{-1} or less of one another working with a large number of host–guest combinations. In equilibration experiments in the same medium at 25 °C with 9·LiPic as the starting complex and **6** or **7** as the acceptor host, $[AG]_i/[B]_i$ values were varied between 0.69 and 5.0 to give K_a values that lay between 0.93×10^{12} and 2.9×10^{12} M^{-1} ($(K_a)_{av} = 1.7 \pm 0.5 \times 10^{12}$ M^{-1} and $-\Delta G° = 16.7$ kcal mol^{-1}) for 9 binding LiPic.[5] Two different experimentalists were involved in obtaining these values. In the same medium at 25 °C with **10**·NaPic as the initial complex and **6** as the acceptor host, $[AG]_i/[B]_i$ values were varied in three runs between 1.1 and 5.9 (absolute concentrations $\approx 10^{-3}$ M) with only a $-\Delta G°$ change of 0.2 kcal mol^{-1} for **10** binding NaPic.[21] The $-\Delta G°$ values for **6** binding NaPic in the same medium at 25 °C determined by the picrate salt-extraction method was 13.6 kcal mol^{-1} and by a kinetic method was 13.3 kcal mol^{-1}.[5] Two different experimentalists were involved in these completely different types of measurements. The ^1H NMR chemical shifts in $CDCl_3$ of a wide variety of spherands, hemispherands, cryptahemispherands, and chorands, and of their alkali metal and ammonium complexes have been shown not to change as their concentrations were varied from 0.05 to 0.001 M concentration (former papers in this series). These facts, taken in sum, indicate that at the concentrations used, the hosts and their complexes are essentially monomeric at 25 °C in $CDCl_3$ saturated with D_2O. The outside error limits for $-\Delta G°$ values determined by method A we estimate to be ±1 kcal mol^{-1} and for those by method B to be ±1.5 kcal mol^{-1}. In those cases where the results of a single run are reported, less exact runs were made to probe the concentrations required to maximize the sensitivities of the measurements. At least one inexact determination, and in most cases several more, were made which provided $-\Delta G°$ values closer to those reported than the above quoted error limits.

(21) Cram, D. J.; Lein, G. M., unpublished results.

Lewis Acid Catalysis of Photochemical Reactions. 4. Selective Isomerization of Cinnamic Esters[1]

Frederick D. Lewis,* Joe D. Oxman, Lester L. Gibson, Hilary L. Hampsch, and Suzanne L. Quillen

Contribution from the Department of Chemistry, Northwestern University, Evanston, Illinois 60201. *Received July 8, 1985*

Abstract: The spectroscopic properties and photoisomerization reactions of several (*E*)- and (*Z*)-cinnamic esters, bis cinnamic esters, and model esters and lactones in the presence and absence of Lewis acids have been investigated. The use of Lewis acids such as BF_3 or $EtAlCl_2$ results in enhanced photoisomerization efficiency and a shift in the photoequilibrium toward the thermodynamically less stable *Z* isomer. Enhanced $E \rightarrow Z$ photoisomerization results from selective excitation of ground-state ester–Lewis acid complexes. These complexes have been characterized by ^1H NMR, ultraviolet, and fluorescence spectroscopies. The equilibrium constants for complexation are dependent upon both the electron donor strength of the ester and its conformational mobility. These factors also determine the magnitude of the red shifts in the electronic absorption spectra observed upon complexation. Enhanced $E \rightarrow Z$ photoisomerization upon complex formation is a consequence of selective excitation of the *E* vs. *Z* complex, more efficient isomerization of the excited *E* vs. *Z* complex, and larger equilibrium constants for complexation of *E* vs. *Z* esters. The photoequilibria obtained for bis cinnamic esters are highly enriched in the *Z,Z* and *Z,E* isomers in accord with independent isomerization of the two cinnamate groups; however, in the case of 1,3-trimethylenebis(cinnamate), two-bond isomerization of the *E,E* to *Z,Z* isomer is observed at low conversions.

Photoisomerization presents the only direct method for contrathermodynamic $E \rightarrow Z$ isomerization of olefins.[2,3] Synthetic applications[4] of this method have been limited by its reversible nature, which, in the absence of other reactions, leads to a

0002-7863/86/1508-3005$01.50/0